Computer Simulation of Diffusion in Multiphase Systems

ANDERS ENGSTRÖM, LARS HÖGLUND, and JOHN ÅGREN

A general model to treat multicomponent diffusion in multiphase dispersions is presented. The model is based on multicomponent diffusion data and basic thermodynamic data and contains no adjustable parameters. No restriction is placed on the number of components or phases that take part in the calculations, as long as the necessary thermodynamic and kinetic data are available. The new model is implemented into the DICTRA software, which makes use of THERMO-CALC to handle the thermodynamics. The model is applied to carburization of Ni alloys and heat treatment of welded joints between dissimilar materials. In both cases, the diffusion is accompanied by carbide formation or dissolution. A good agreement between experiments and calculations is found, despite the fact that no adjustable parameters are needed.

I. INTRODUCTION

IN binary diffusion couples, new phases form as layers perpendicular to the direction of diffusion. The growth of such layers will then be controlled by diffusion through the layers themselves. When three or more components take part in a diffusion process, the situation becomes more complex, and new phases may form also as dispersed particles in a matrix. For example, when a pure metal is oxidized, an oxide layer forms on the surface, whereas upon oxidizing an alloy, discrete oxide particles may form in the interior; so-called internal oxidation.[1] A similar behavior is observed during carburizing and nitriding.

If a binary Fe-C steel is decarburized at a temperature below A_1, a ferritic layer will form at the surface and grow into the steel. The fraction of cementite will drop from its initial value to zero within a very thin layer, and on a micrograph, there appears to be a sharp boundary between the two-phase mixture and the surface layer. The overall C content drops more or less discontinuously at this boundary. On the other hand, when a high-alloy steel is decarburized, there will be gradual change in the volume fraction of carbides as we approach the surface from the interior, and there will be a continuous variation in C content.

The difference in behavior is related to the Gibbs phase rule, which states that under isobaric and isothermal conditions, there are no degrees of freedom left in a binary alloy when two phases coexist at equilibrium. If the interparticle spacing is small compared to the distances over which diffusion occurs, there can be no chemical-potential gradients to cause long-range diffusion in a binary two-phase mixture.

Recently, models for diffusion in one-phase multicomponent systems[2] and diffusion-controlled growth of layers and individual particles[3] were developed and implemented as a subroutine package called DICTRA. The main ambition was to base the treatment on only basic thermodynamic and kinetic data obtained independently of the transformation under consideration. The purpose of the present report is to treat the problem of long-range diffusion through multiphase structures with the same ambition.

This problem has been tackled by several authors over the years. Ågren,[4] when treating C diffusion in tool steels, reduced the problem to an ordinary one-phase diffusion problem by introducing an effective diffusion coefficient. The effective diffusion coefficient was calculated from the C diffusivity in the matrix and the thermodynamic properties of the multiphase system only. In general, the effective diffusivity will be concentration dependent and numerical methods are needed to solve the diffusion equation. Quite recently, Morral *et al.*[5] presented a similar approach, but in addition, they suggested that one should simply evaluate the quantities needed in the calculation from a diffusion experiment. Such an approach is of course always possible but must be considered as less useful because it requires a new experiment if the temperature or the alloy composition is changed a little.

Bongartz *et al.*,[6] when treating carburization of high-temperature alloys, adopted a more elaborate numerical technique which made use of some thermodynamic and kinetic data. They assumed that the carbides are always in equilibrium with the matrix, and after each time-step, the amount of C tied up in the particles was calculated by means of equilibrium constants for each carbide and then subtracted from the C content of the matrix. However, their calculations were based on a number of simplifying assumptions; *e.g.*, the diffusion coefficient of C was assumed to be constant and adjusted to obtain a best fit and no cross terms were included. Somewhat later, Farkas and Ohla,[7] with a similar approach, treated the same problem taking the cross terms into account and adjusted only the assumed concentration-independent diffusion coefficient of C in order to obtain a best fit to the experimental curve. In a recent article, Bongartz *et al.*[8] presented a refined model, and a very good agreement between calculations and experimental data was reported. However, a closer examination of the report reveals that the major part of the thermodynamic and diffusivity data needed in the calculations were actually adjusted in order to fit the experimental data. Since both thermodynamic[9] and diffusion[10] data are now available from independent sources, it is tempting to combine these in order to examine how good the

ANDERS ENGSTRÖM and LARS HÖGLUND, Graduate Students, and JOHN ÅGREN, Professor, are with the Department of Materials Science and Engineering, Division of Physical Metallurgy, Royal Institute of Technology, S-100 44 Stockholm, Sweden.

Manuscript submitted March 29, 1993.

agreement between calculations and experiments is without making use of any adjustable parameters.

In this report, we will apply concentration-dependent diffusion coefficients and develop a general model for multicomponent diffusion in multiphase dispersions. For the equilibrium calculations, we will use a full Gibbs energy minimization method, as available in the THERMO-CALC system,[11] rather than equilibrium constants. Such a procedure is more general than the dilute solution formalism based on Wagnerian interaction coefficients and works very well over the whole concentration range. Full account is taken for the variable composition of the various carbides.

For a simulation, a complete thermodynamic description of the system is needed, *i.e.*, a description from which the multicomponent phase diagram may be calculated. Such descriptions are available within the THERMO-CALC system[11] and will be used in the present work. In addition, a complete set of multicomponent diffusive mobilities is needed. At present, such data are available for a few systems only. In this report, we have applied the data from Jönsson.[10,12]

II. THE MODEL

As in the methods of Bongartz *et al.*[6,8] and Farkas and Ohla,[7] the present calculation is divided into two steps, diffusion and equilibrium. The two steps will now be described separately.

A. *The Diffusion Step*

Only volume diffusion is considered, and the diffusion is assumed to take place in a matrix phase. However, the normal diffusion paths are partly blocked by the precipitates, and thus the effective diffusion distance is bigger than if there were no particles. It is common to account for this effect by multiplying the diffusivity with a so-called labyrinth factor, which has a value between zero and unity. The labyrinth factor depends on the fraction of particles, their morphology, and the size distribution function. For some simple shapes and distributions, *e.g.*, a random distribution of equally sized noninteracting spheres, the labyrinth factor may be calculated exactly.[13] However, in general, an analytical solution is not possible. In the present work, the particles are present both as interior particles, some elongated and some fairly spheroidal, and as grain-boundary precipitates. It thus seems that one should expect a stronger effect than in the case of the equally sized noninteracting spheres. On the other hand, one should expect a weaker effect than if all particles were platelets with an aspect ratio of 1/4, arranged in order to block the diffusion, a case which has also been solved analytically.[13] These simple considerations give estimates of the upper and lower bounds of the labyrinth factor. It is found that a labyrinth factor f^2, where f is the volume fraction of the matrix, falls in the middle between these upper and lower bounds for $f > 0.7$ but lower than the lower bound for $f < 0.5$. However, when $f < 0.5$, a more or less continuous network of grain-boundary carbides is formed, and one may actually expect a stronger effect than in the case of platelets. Quadakkers *et al.*[14] have studied the carburization of both single crystals and polycrystals of Ni-25 wt pct Cr alloys. In the latter case, a large portion of the carbides form along grain boundaries, whereas in the former case, there are of course only interior carbides. The C profiles in these two cases were fairly similar, but the case depth in the polycrystalline was somewhat lower than in the single crystalline material, indicating a difference in the labyrinth factor. For these reasons and for the sake of simplicity, we have thus chosen f^2, which seems to yield a reasonable behavior.

The diffusion equations are solved with a numerical method for coupled diffusion equations developed by Ågren.[15] Necessary kinetic data were taken from the multicomponent diffusivities recently assessed by Jönsson.[12]

B. *The Equilibrium Step*

It is convenient to use the concentration variable u_k defined as

$$u_k = \frac{x_k}{\sum_{j \in s} x_j} \qquad [1]$$

where x is the normal mole fraction and the summation is taken over the substitutional elements only. Under the assumption that all the substitutional elements have the same partial molar volume in all phases and that the partial molar volume of the interstitials may be neglected, the volume fraction of a phase α will be equal to the mole fraction f^α including only the substitutional elements; *i.e.*,

$$f^\alpha = \frac{\sum n_j^\alpha}{\sum n_j^{tot}} \qquad [2]$$

where n_j^α is number of moles of component j in the α phase and n_j^{tot} is the total number of moles of component j. Again, the summations are performed over the substitutional elements only. The assumption that all the substitutional elements have the same partial molar volume in all phases may seem rather rough for those cases where detailed information is available, but it should be understood that provided that volume differences do not give rise to stresses, they should not affect the diffusion. In general, we would expect stresses to relax at high temperatures where the substitutional elements are mobile.

During the diffusion step, only the composition of the matrix is changed; the fraction and the composition of the various particles remain unaffected. As a result of the composition change in the matrix, there is a change in the overall composition. The overall composition in each gridpoint after the diffusion step is given by the following:

$$u_k^{tot'} = u_k^{tot} + f^\alpha (u_k^{\alpha'} - u_k^\alpha) \qquad [3]$$

where α now stands for the matrix and $u_k^{tot'}$ is the overall u fraction of component k, after a diffusion step, u_k^{tot} is

the overall u fraction of component k before a diffusion step, $u_k^{\alpha'}$ is the u fraction of component k in the matrix phase after a diffusion step, u_k^{α} is the u fraction of component k in the matrix phase before the diffusion step, and f^{α} is the volume fraction of the matrix phase.

The time-step in the diffusion calculations is assumed long enough for all the precipitates to react until equilibrium is reached locally. After the diffusion step, the equilibrium corresponding to the new overall composition is calculated at each gridpoint. The equilibrium calculations are made using THERMO-CALC.[11] After the equilibrium calculations, the u fractions of the different elements in the matrix u_k^{α} are updated and the diffusion step is repeated. This procedure has now been implemented into the DICTRA package.[3]

III. EXAMPLE OF SIMULATIONS

The computer program is quite general, and it is possible to make simulations of a number of different problems without changing the program, provided that the necessary thermodynamic and kinetic data are known. In this report, we will give examples of simulations on two different problems. First, we will treat carburization of the Ni-based alloys treated by Bongartz *et al.*,[8,14,16] and Christl *et al.*[17] and the simultaneous carburization and oxidation of Cr in Fe-Cr-Ni alloys, as studied by Grabke *et al.*[18] We will then consider the annealing of weldments of dissimilar Cr alloys treated earlier by Buchmayr and Kirkaldy.[19]

A. *Carburization of Ni-Based Alloys*

Calculations were performed for a number of different alloy compositions, *i.e.*, Ni-25 wt pct Cr, Ni-30 wt pct Cr, Ni-19 wt pct Cr-49 wt pct Fe, and Ni-25 wt pct Cr-44 wt pct Fe. Boundary conditions and global conditions were chosen in accordance with the detailed experimental information given in References 8, 14, 16, and 17. Hence, most of the simulations were done at 850 °C for 1000 hours with the assumption of a constant surface C activity, $a_C = 1$ relative to graphite. One calculation was performed with a C activity $a_C = 0.39$ to allow a comparison with experimental information from Reference 17. In all simulations, it was assumed that no oxide layer could form at the surface. Thermodynamic data for the Fe-Ni-Cr-C system were taken from a recent assessment by Lee.[9] Figures 1 through 5 show examples of simulations done for the aforementioned alloy compositions. The experimental information from References 8, 14, and 16 concerns the overall C concentration profiles and the fraction of carbides and from Reference 17 the Cr content of the matrix. In order to calculate volume fractions from the molar fractions given by the calculations, molar volumes of the various phases are needed. These were calculated from the lattice parameter data in Reference 20. Approximating the carbide molar volumes with the molar volumes of Cr_3C_2 and Cr_7C_3, we obtain 9.3 and 8.3 cm^3/mol metal atom, respectively. In a similar way, the molar volume of the fcc phase was estimated to be 6.7 cm^3/mol metal atom. As can be seen, the agreement between calculations and experiments in Ni-25 wt pct Cr and Ni-30 wt pct Cr alloys, (Figures 1 and 2) is

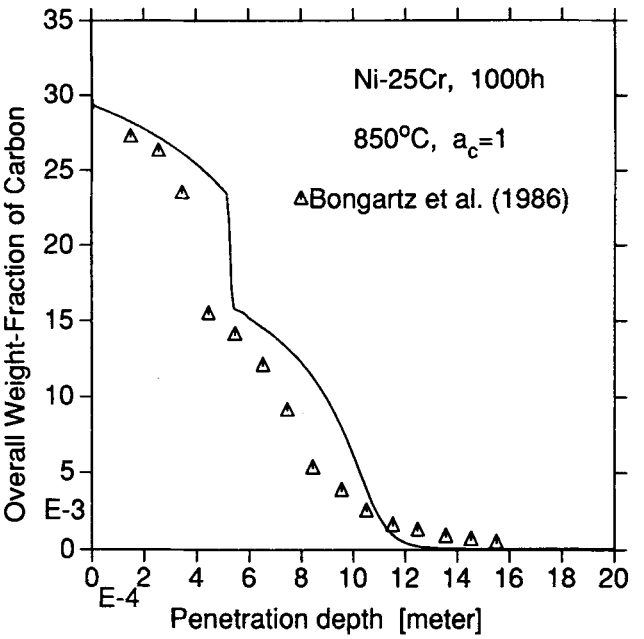

(*a*)

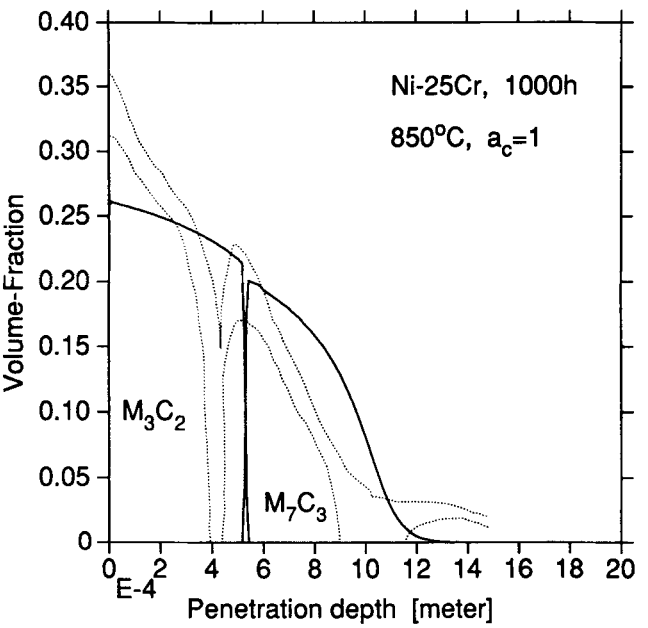

(*b*)

Fig. 1—(*a*) Total C concentration in weight fraction *vs* penetration depth for an Ni-25 wt pct Cr alloy after carburization for 1000 h at 850 °C with a constant surface C activity, $a_c = 1$. Symbols: experimental data from Ref. 16. (*b*) Volume fraction of the precipitated carbides *vs* penetration depth for the Ni-25 wt pct Cr alloy. Solid line: calculated. Dotted lines: experimental data from Ref. 14.

quite satisfactory, considering the fact that no adjustable parameters have been used in the calculations. The main discrepancy is that Bongartz *et al.*[8,14,16] report formation of small amounts of $M_{23}C_6$ at very low C contents in the Ni-25 wt pct Cr alloy. However, formation of $M_{23}C_6$ in a Ni-25 wt pct Cr alloy cannot be reconciled with the thermodynamic information available for this temperature. Moreover, the metallographic evidence[16] for formation of this carbide in that alloy does not seem very

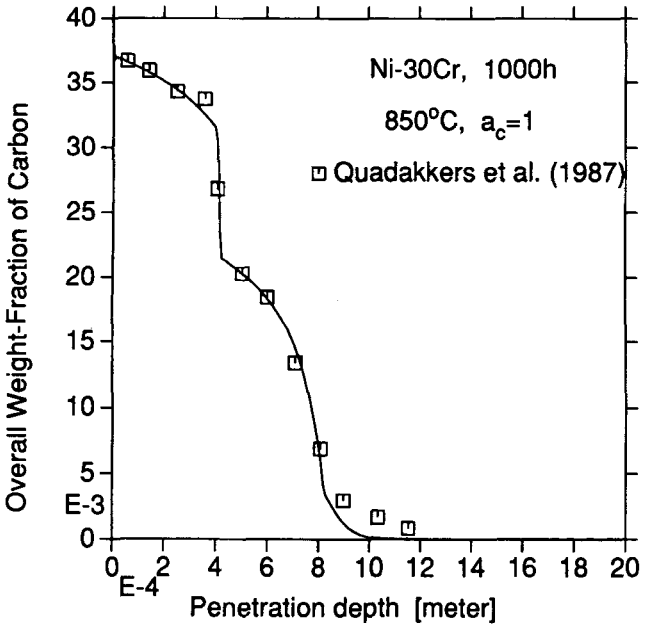

(*a*)

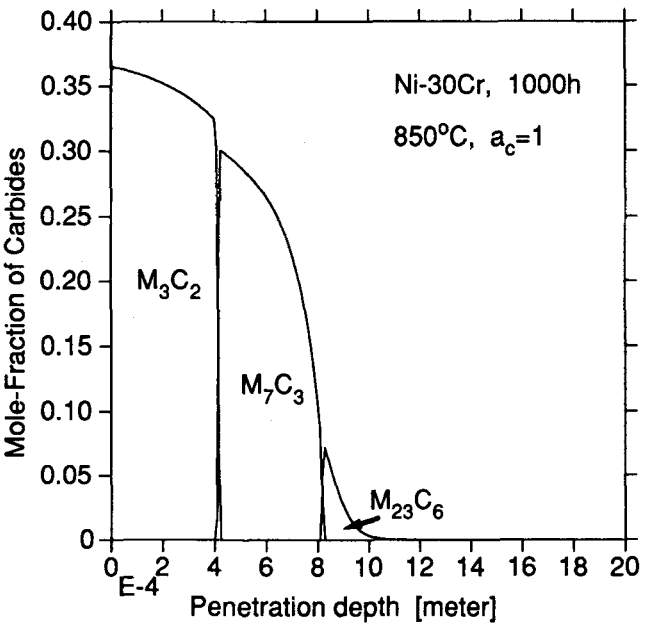

(*b*)

Fig. 2—(*a*) Total C concentration in weight fraction *vs* penetration depth for an Ni-30 wt pct Cr alloy after carburization for 1000 h at 850 °C with a constant surface C activity, a_c = 1. Symbols: experimental data from Ref. 14. (*b*) Mole fraction of the precipitated carbides *vs* penetration depth for the Ni-30 wt pct Cr alloy.

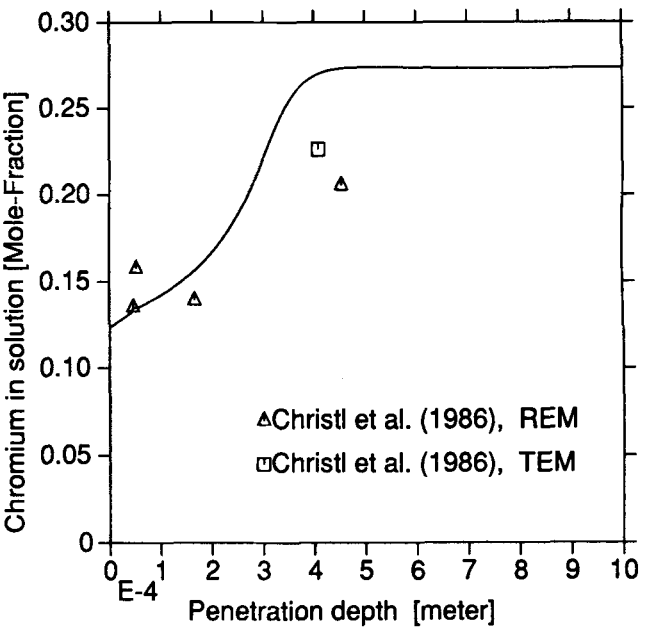

Fig. 3—Chromium content of matrix as x_{Cr} *vs* penetration depth for an Ni-25 wt pct Cr alloy after carburization for 150 h at 850 °C with a constant surface C activity, a_c = 0.39. Symbols: experimental data from Ref. 17.

strong. The agreement between measured and calculated matrix compositions is satisfactory (Figure 3). Figures 4 and 5 show calculations for two alloys also containing Fe. The agreement between calculated and measured C profiles is remarkably good.

Grabke *et al.*[18] investigated carburization in the temperature interval 800 °C to 1200 °C of commercial Fe-25 wt pct Cr-20 wt pct Ni alloys with initially 0.42 wt pct C, 1.47 wt pct Si, and 0.98 wt pct Mn. In their experiment, the O potential was high enough to cause formation of Cr-rich oxides at the surface, giving a protective layer that greatly increased the carburization resistance of the alloy. However, at temperatures above 1050 °C, the oxide was no longer stable and transformed to an external M_7C_3 layer, and hence the protection from the oxide layer was lost. During carburization of these alloys at 1100 °C, the formation of Cr_2O_3 at the surface of the alloy will cause a depletion of Cr close to the surface. The M_7C_3 carbide forming from the oxide seems to form a continuous surface layer in the micrographs presented by Grabke *et al.* The resulting concentration gradients will cause diffusion of Cr from the interior toward the surface. At the same time, C is added at the surface and diffuses through the M_7C_3 layer into the metal. It is thus evident that even if the C activity in the surrounding media is high and close to unity, it must be lower at the M_7C_3/metal interface because some driving force is needed for the C diffusion through the M_7C_3 layer. In principle, one should take into account the growth of the M_7C_3 layer governed by the Cr diffusion and diffusion of C through this layer at the same time as the diffusion in the metal. However, owing to lack of data, a simpler approach was taken in the present study. It was assumed that the Cr content in the metal in local equilibrium with the surface layer was zero. The C activity at the interface was adjusted until the best agreement between the experimental and the theoretical C concentration profiles was obtained. For the rest of the components, a closed system was assumed. The additional thermodynamic data involving Si and Mn were taken from the THERMO-CALC data bank.[11] Figures 6(a) and (b) depict the experimental C concentration profile with two calculated profiles. The dashed curve was calculated assuming the C activity at the M_7C_3/metal interface is unity, *i.e.*, no driving force is needed for diffusion through the M_7C_3 layer. The solid

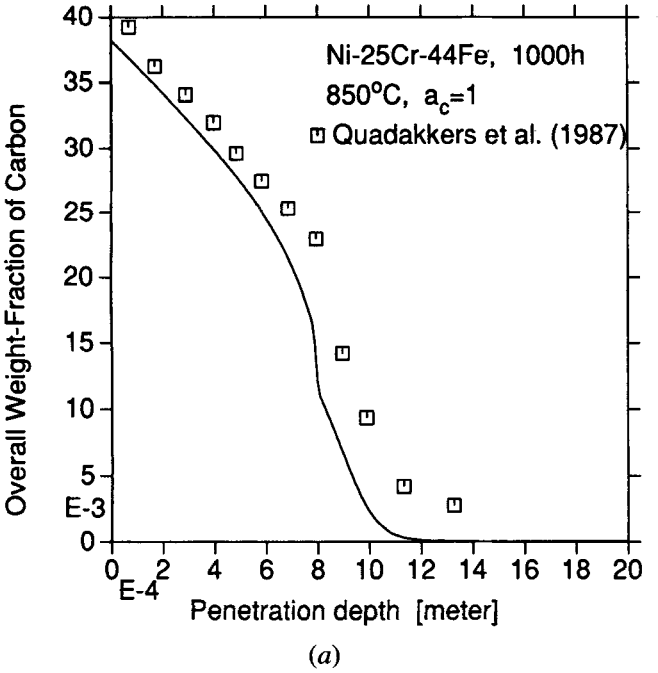

(*a*)

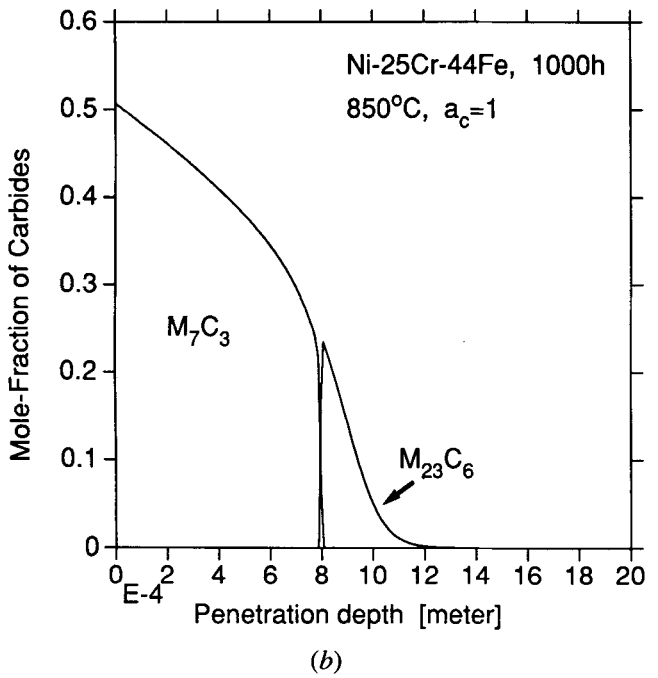

(*b*)

Fig. 4—(*a*) Total C concentration in weight fraction *vs* penetration depth for an Ni-25 wt pct Cr-44 wt pct Fe alloy after carburization for 1000 h at 850 °C with a constant surface C activity, a_c = 1. Symbols: experimental data from Ref. 14. (*b*) Mole fraction of the precipitated carbides *vs* penetration depth for the Ni-25 wt pct Cr-44 wt pct Fe alloy.

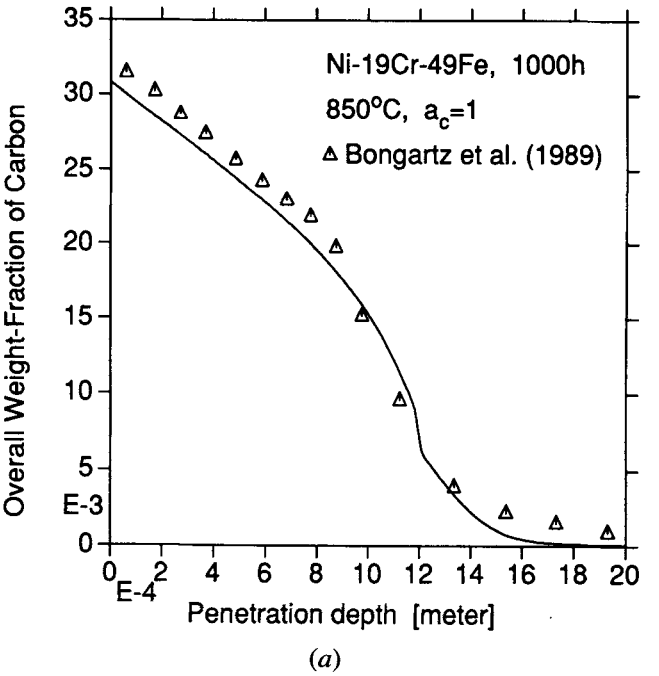

(*a*)

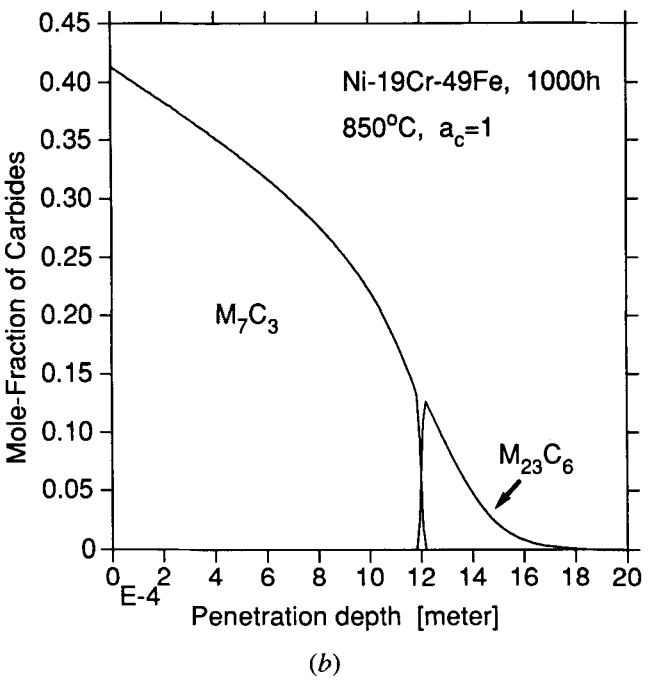

(*b*)

Fig. 5—(*a*) Total C concentration in weight fraction *vs* penetration depth for an Ni-19 wt pct Cr-49 wt pct Fe alloy after carburization for 1000 h at 850 °C with a constant surface C activity, a_c = 1. Symbols: experimental data from Ref. 8. (*b*) Mole fraction of the precipitated carbides *vs* penetration depth for the Ni-19 wt pct Cr-49 wt pct Fe alloy.

line, which is in satisfactory agreement with the experimental profile, was calculated assuming a C activity at the M_7C_3/metal interface is 0.45 relative to graphite. A Δa_C = 0.55 is thus needed for the diffusion through the M_7C_3 layer. Close to the M_7C_3/metal interface there is a thin carbide-free layer caused by depletion of Cr which is a strong carbide stabilizer. It should be noticed that the calculated thickness of the carbide-free zone is in very good agreement with the observed one. Below the carbide-free zone, there is internal carbide formation of first M_7C_3 and further in $M_{23}C_6$. It may also be noticed that the calculated carburizing depth is in satisfactory agreement with the one indicated by the experimental C contents. However, the calculations predict a sharp peak in the C content at the $\gamma/\gamma + M_7C_3$ interface. This peak cannot be seen in the experiments, which seem to show a more gradual decrease in C content toward the surface. This discrepancy can partly but not fully be explained

by the fact that the C content was measured from a chemical analysis of rather coarse turnings.

B. *Annealing of a Mismatched Chromium Alloy Weldment*

During postweld heat treatment of 1 wt pct CrMoV and 12 wt pct CrMoV weldments, microstructural changes occur in the weld. The low-alloy steel will be decarburized, and the high-alloy filler metal will be carburized. The change in C content is accompanied by important structural changes and changes of the mechanical properties. From a practical point of view, it is thus important to understand and to predict the changes. Figures 7 and 8 show simulations with Cr as the only alloying element. The C content on the low-alloy side was 0.17 wt pct and on the high-alloyed side 0.2 wt pct. The calculations were performed for the temperatures 680 °C and 730 °C for 2 and 10 hours, respectively.

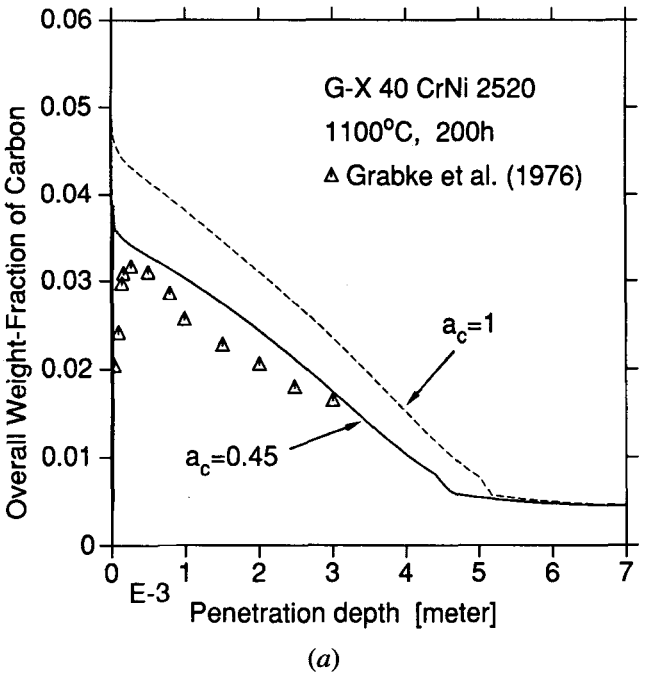

(*a*)

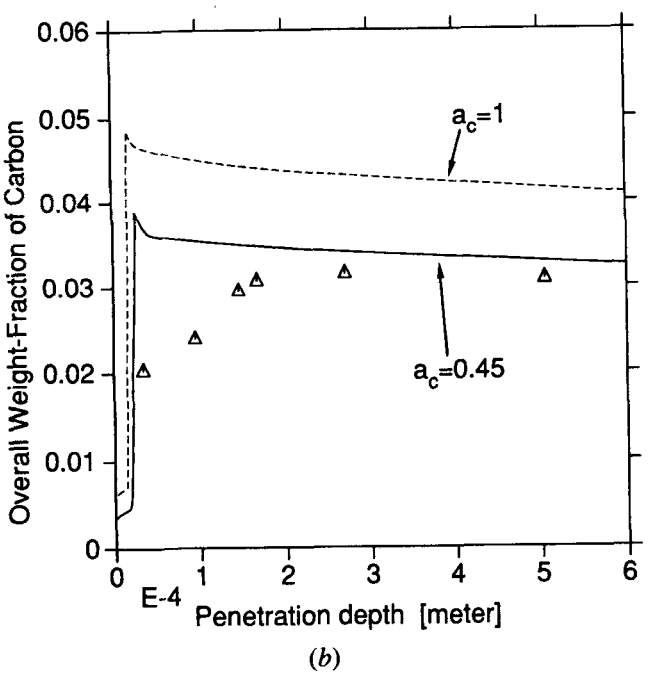

(*b*)

Fig. 6—(*a*) Total C concentration in weight fraction *vs* penetration depth for a Fe-25 wt pct Cr-20 wt pct Ni alloy with initially 0.42 wt pct C, 1.47 wt pct Si, and 0.98 wt pct Mn after carburization for 200 h at 1100 °C with a constant surface C activity, a_c = 0.45 (solid line) and a_c = 1 (dashed line). Symbols: experimental data from Ref. 18. (*b*) Same as (a) but different scale on *x*-axis.

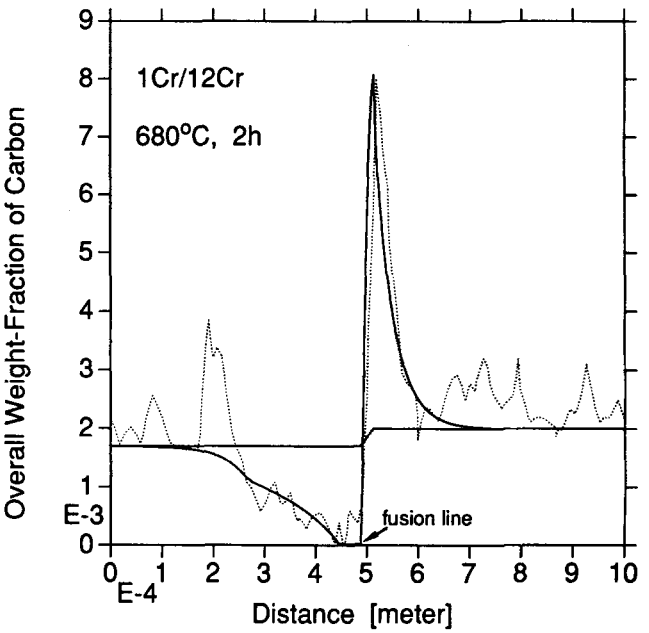

(*a*)

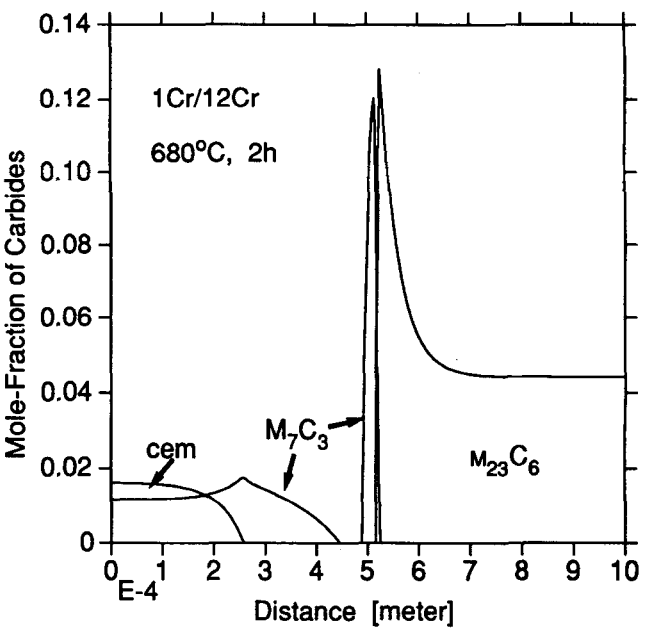

(*b*)

Fig. 7—(*a*) Profile of total C concentration in weight fraction in the 1 wt pct Cr/12 wt pct Cr couple after postweld heat treatment at 680 °C for 2 h. Solid line: calculated. Dotted line: experimental data from Ref. 19. (*b*) Mole fraction of carbides in the weldment after postweld heat treatment at 680 °C for 2 h.

Thermodynamic data of the Fe-Cr-C system were taken from Reference 9, and cementite, M_7C_3, and $M_{23}C_6$ took part in the calculations. These carbides have also been experimentally observed in the weldments.[21] The calculations are compared with experimental data from Reference 19 (dashed lines in Figures 7(a) and 8(a)). Buchmayr and Kirkaldy only reported the concentration profiles obtained by electron microprobe analysis as cts/s. Their profiles were recalculated into ordinary concentration profiles, assuming the C content is a linear function of the measured profile and using the C content of the 12 wt pct Cr steel and the very low C content of the ferrite layer in the 1 wt pct Cr steel close to the joint as standards. The agreement between calculations and measurements should be considered as satisfactory. It should be mentioned that the C concentration at the peak is a function not only of time and temperature but of the initial Cr gradient present. This gradient is developed during the welding and depends on the welding procedure. In principle, it is possible to simulate the cooling with the DICTRA package and then enter the concentration profiles obtained from this simulation as the starting profiles for simulation of the postweld heat treatment. However, for simplicity, and because no information on the welding procedure in this particular case was found, the initial Cr gradients were assumed constant. Figure 9 shows how the C peak concentration depends on the Cr gradient initially present in the weldment. The other simulation conditions were identical to those in Figure 7. It is encouraging to notice that the experimental information from Reference 19 indicates that the Cr gradient extends over approximately 60 μm, which gives an inverse Cr gradient of 5.45 μm/pct Cr. From Figure 9, it can be seen that the C content at the peak for this gradient is around 0.75 wt pct which is in very good agreement with observed values.

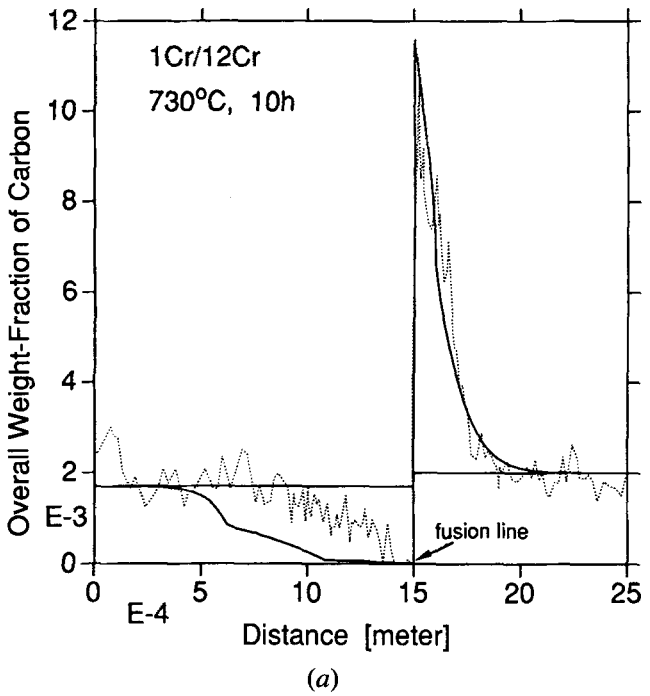

(*a*)

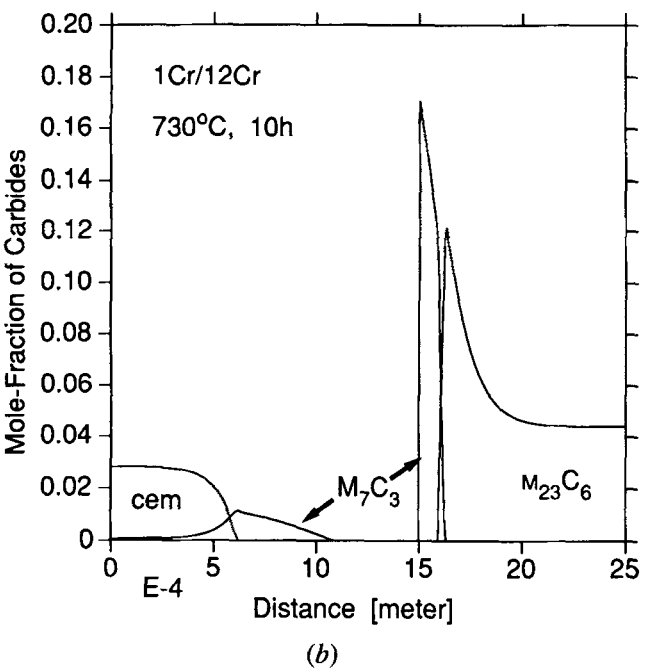

(*b*)

Fig. 8—(*a*) Profile of total C concentration in weight fraction in the 1 wt pct Cr/12 wt pct Cr couple after postweld heat treatment at 730 °C for 10 h. Solid line: calculated. Dotted line: experimental data from Ref. 19. (*b*) Mole fraction of carbides in the weldment after postweld heat treatment at 730 °C for 10 h.

C. *Effect of the Time-step*

It should be emphasized that the results in all calculations depend to some extent on the time-step chosen. Although the time-step is controlled by an automatic procedure, the user may prescribe a maximum size of the time-step. If a big maximum time-step is allowed, the calculations will run fast, but the results will be less accurate. As the maximum timestep is decreased, the results become gradually less dependent on the time-step.

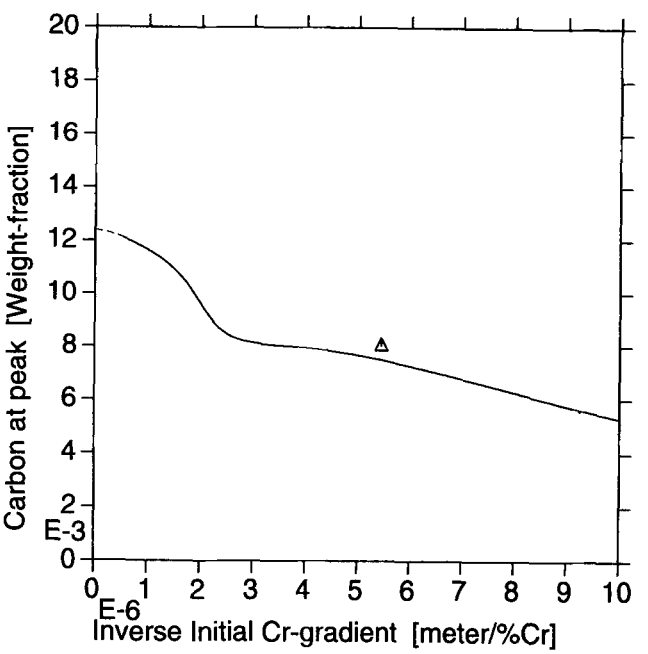

Fig. 9—Weight fraction of C at peak after postweld heat treatment at 680 °C for 2 h as function of the initially present Cr gradient. Dashed line: extrapolation. Symbol: experimental data from Ref. 19.

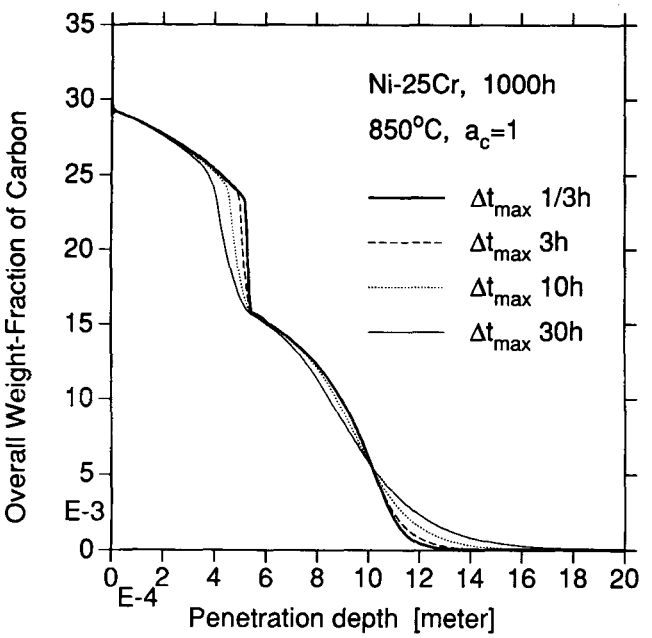

Fig. 10—The C profile in Fig. 1(a) for different maximum time-step.

Figure 10 shows how the calculation in Figure 1 depends on the maximum allowed time-step. The computational time in Figure 10 varies between 15 minutes to 1 day on a Sparc station 2. The reason for this dependence on the maximum time-step is that large time-steps will cause high supersaturations in the matrix phase during the diffusion-step. Another cause to the time-step dependence is the explicit nature of Eq. [3].

IV. SUMMARY AND CONCLUSIONS

A general model to treat diffusion in multiphase dispersions has been presented. The model makes use of basic thermodynamic and kinetic data without any adjustable parameters. No restriction is placed on the number of components or phases that take part in the calculations, as long as the necessary thermodynamic and kinetic data are available. The good agreement between numerical and experimental results shows that this physically based model is capable of predicting the complex diffusion processes that take place in a multicomponent, multiphase system.

ACKNOWLEDGMENTS

The authors would like to thank Dr. Björn Jönsson for stimulating discussions. This work is part of a project sponsored by the Swedish Research Council for Engineering Sciences.

REFERENCES

1. R.A. Rapp: *Acta Metall.*, 1961, vol. 9, pp. 730-41.
2. J.-O. Andersson and J. Ågren: *J. Appl. Phys.*, 1992, vol. 72, pp. 1350-55.
3. J.-O. Andersson, L. Höglund, B. Jönsson, and J. Ågren: *Fundamentals and Applications of Ternary Diffusion*, G.R. Purdy, ed., Pergamon Press, New York, NY, 1990, pp. 153-63.
4. J. Ågren: *Scand. J. Metall.*, 1981, vol. 10, pp. 134-40.
5. J.E. Morral, B.M. Dupen, and C.C. Law: *Metall. Trans. A*, 1992, vol. 23A, pp. 2069-71.
6. K. Bongartz, D.F. Lupton, and H. Schuster: *Metall. Trans. A*, 1980, vol. 11A, pp. 1883-93.
7. D. Farkas and K. Ohla: *Oxid. Met.*, 1983, vol. 19, pp. 99-115.
8. K. Bongartz, W.J. Quadakkers, R. Schulten, and H. Nickel: *Metall. Trans. A*, 1989, vol. 20A, pp. 1021-28.
9. Byeong-Joo Lee: Royal Institute of Technology, Stockholm, unpublished research, 1991.
10. B. Jönsson: Royal Institute of Technology, Stockholm, unpublished research, 1992.
11. B. Sundman, B. Jansson and J.-O. Andersson: *CALPHAD*, 1985, vol. 9, pp. 153-90.
12. B. Jönsson: Internal Report, Trita-Mac-0504, Royal Institute of Technology, Stockholm, 1992.
13. R.L. McCullough: *Compos. Sci. Technol.*, 1985, vol. 22, pp. 3-21.
14. W.J. Quadakkers, R. Schulten, K. Bongartz, and H. Nickel: *10th Int. Conf. on Metal Corrosion*, Madras, India, Nov. 1987, Trans Tech Publishers, Aedermannsdorf, pp. 1737-46.
15. J. Ågren: *J. Phys. Chem. Solids*, 1982, vol. 43, pp. 385-91.
16. K. Bongartz, R. Schulten, W.J. Quadakkers, and H. Nickel: *Corrosion*, 1986, vol. 42, pp. 390-97.
17. W. Christl, H.J. Christ, and H.G. Sockel: *Werkst. Korros.*, 1986, vol. 37, pp. 385-90 and 437-43.
18. Von H.J. Grabke, U. Gravenhorst and W. Steinkusch: *Werkst. Korros.*, 1976, vol. 27, pp. 291-96.
19. B. Buchmayr and J.S. Kirkaldy: *Fundamentals and Application of Ternary Diffusion*, G.R. Purdy, ed., Pergamon Press, New York, NY, 1990, pp. 164-72.
20. W.B. Pearson: *Handbook of Lattice Spacings and Structures of Metals and Alloys*, Pergamon Press, New York, NY, 1958.
21. B. Buchmayr, H. Cerjak, J.S. Kirkaldy, and M. Witwer: *2nd Int. Conf. Trends in Welding Research*, Gatlingburg, TN, 1989, ASM INTERNATIONAL, Materials Park, OH, 1990, pp. 237-42.